JLA *Journal of Lipid and Atherosclerosis*

Original Article

Check for updates

Correspondence to
Je-Hyun Yoon
Department of Biochemistry and Molecular Biology, Medical University of South Carolina, 173 Ashley Avenue, Charleston, SC 29425, USA.
Email: yoonje@musc.edu

Joe R. Delaney
Department of Biochemistry and Molecular Biology, Medical University of South Carolina, 173 Ashley Avenue, Charleston, SC 29425, USA.
Email: delaneyj@musc.edu

ORCID iDs
Seungbeom Ko
https://orcid.org/0000-0002-8457-3134
Eunbyul Yeom
https://orcid.org/0000-0003-0598-6844
Marina Howard-McGuire
https://orcid.org/0000-0002-4328-6569
Nathan T. Millison
https://orcid.org/0000-0003-1131-5713
Changhan Lee
https://orcid.org/0000-0003-0327-4712

Profiling of RNA-binding Proteins Interacting With Glucagon and Adipokinetic Hormone mRNAs

Seungbeom Ko ,[1] Eunbyul Yeom ,[2] Yoo Lim Chun,[3] Hyejin Mun,[1] Marina Howard-McGuire ,[1] Nathan T. Millison ,[1] Junyang Jung,[4] Kwang-Pyo Lee,[5] Changhan Lee ,[6] Kyu-Sun Lee ,[2] Joe R. Delaney ,[1] Je-Hyun Yoon [1]

[1]Department of Biochemistry and Molecular Biology, Medical University of South Carolina, Charleston, SC, USA
[2]Neurophysiology and Metabolism Research Group, Korea Research Institute of Bioscience and Biotechnology (KRIBB), Daejeon, Korea
[3]Department of Biomedical Science, Graduation School, Kyung Hee University, Seoul, Korea
[4]Department of Anatomy and Neurobiology, College of Medicine, Kyung Hee University, Seoul, Korea
[5]Aging Research Center, Korea Research Institute of Bioscience and Biotechnology (KRIBB), Daejeon, Korea
[6]Leonard Davis School of Gerontology, University of Southern California, Los Angeles, CA, USA

ABSTRACT

Objective: Glucagon in mammals and its homolog (adipokinetic hormone [AKH] in *Drosophila melanogaster*) are peptide hormones which regulate lipid metabolism by breaking down triglycerides. Although regulatory mechanisms of glucagon and AKH expression have been widely studied, post-transcriptional gene expression of glucagon has not been investigated thoroughly. In this study, we aimed to profile proteins binding with *Gcg* messenger RNA (mRNA) in mouse and *Akh* mRNA in Drosophila.
Methods: Drosophila Schneider 2 (S2) and mouse 3T3-L1 cell lysates were utilized for affinity pull down of *Akh* and *Gcg* mRNA respectively using biotinylated anti-sense DNA oligoes against target mRNAs. Mass spectrometry and computational network analysis revealed mRNA-interacting proteins residing in functional proximity.
Results: We observed that 1) 91 proteins interact with *Akh* mRNA from S2 cell lysates, 2) 34 proteins interact with *Gcg* mRNA from 3T3-L1 cell lysates. 3) *Akh* mRNA interactome revealed clusters of ribosomes and known RNA-binding proteins (RBPs). 4) *Gcg* mRNA interactome revealed mRNA-binding proteins including Plekha7, zinc finger protein, carboxylase, lipase, histone proteins and a cytochrome, Cyp2c44. 5) Levels of *Gcg* mRNA and its interacting proteins are elevated in skeletal muscles isolated from old mice compared to ones from young mice.
Conclusion: *Akh* mRNA in S2 cells are under active translation in a complex of RBPs and ribosomes. *Gcg* mRNA in mouse precursor adipocyte is in a condition distinct from *Akh* mRNA due to biochemical interactions with a subset of RBPs and histones. We anticipate that our study contributes to investigating regulatory mechanisms of *Gcg* and *Akh* mRNA decay, translation, and localization.

Keywords: Glucagon; RNA-binding proteins; Mass spectrometry

Generated by xmlinkpress

Kyu-Sun Lee (iD)
https://orcid.org/0000-0002-4529-5186
Joe R. Delaney (iD)
https://orcid.org/0000-0002-8978-5961
Je-Hyun Yoon (iD)
https://orcid.org/0000-0001-7615-8654

Conflict of Interest

The authors have no conflicts of interest to declare.

Author Contributions

Conceptualization: Yoon JH; Data curation: Yoon JH; Formal analysis: Ko S, Chun YL, Mun H, Howard-McGuire M, Jung J, Lee KS, Delaney JR, Yoon JH; Investigation: Ko S, Yeom E, Chun YL, Mun H, Howard-McGuire M, Millison NT, Jung J, Lee KP, Lee C, Lee KS, Delaney JR; Methodology: Yoon JH; Validation: Ko S, Delaney JR, Yoon JH; Visualization: Delaney JR, Yoon JH; Writing - original draft: Ko S, Yeom E, Chun YL, Delaney JR, Yoon JH; Writing - review & editing: Ko S.

INTRODUCTION

Glucagon in mammals and its homologues in invertebrates, adipokinetic hormone (AKH) are peptide hormones regulating lipid metabolism.[1-6] They mainly function in lipid droplets of adipocytes by promoting break down of lipids from triglycerides (TGs) to a glycerol and three fatty acids.[7-9] In Tobacco hornworm (*Manduca sexta)* fat body adipocytes, AKH is recognized by AKH receptor, activates cyclic adenosine monophosphate-dependent protein kinase (PKA), and then induces phosphorylation of lipid storage droplet protein-1 (LSD1) subsequently.[1,10] Once phosphorylated, LSD1 activates TG-lipase hydrolyzing TGs in lipid droplet, a process called lipolysis.[11,12] Similarly, Glucagon also influences lipolysis in human and mouse adipose tissues.[2] Glucagon activates PKA to induce phosphorylation of hormone sensitive lipase (HSL) and perilipins (P).[2,13] P activates adipose triglycerol lipase (ATGL) by dissociation of an adaptor protein, comparative gene identification 58.[14] Activated ATGL and HSL induce lipolysis of TGs in lipid droplet[2,15] Overall lipid metabolic pathways are similar to each other in mammals and invertebrates.

To keep the homeostasis of glucose levels, production and release of Glucagon and AKH are under active control in transcriptional and post-transcriptional levels by external stimuli including insulin in mammals and insulin-like peptide in Drosophila (DILP).[16,17] Physical interaction between DILP1 and DILP2 regulates *Akh* messenger RNA (mRNA) and protein level in Drosophila.[16] Similarly, glucagon gene (*Gcg*) expression is regulated by transcription factors such as PAX6, MAF and FoxA during α-cell differentiation in human.[18-21] PAX6 forms heterodimer with cMAF or MAFB; PAX6/cMAF and PAX6/MAFB complex interact with the promoter region of G1 *Gcg* and induce *Gcg* mRNA transcription in mammals.[19] FoxA also hetero-dimerizes with Pax6[20]; Pax6/FoxA complex regulates steady state level of *Gcg* mRNA and FoxA1 knockout mice died in 12 days after birth due to biosynthetic defect of gluconeogenic enzymes leading to hypoglycemia.[21] Despite numerous studies of Glucagon and *Akh*, post-transcriptional regulatory mechanisms of *Gcg* and *Akh* mRNA are still under investigation. RNA-binding protein HuD was reported to bind 3′-UTR of *Gcg* mRNA in mouse pancreatic islet and mouse glucagonoma αTC1 cell line.[22] Depletion of HuD using siRNAs decreased level of pro-glucagon in αTC1 cells whereas *Gcg* mRNA levels did not change significantly.[22] Overall, there are a handful of studies in regulation of Gcg and AKH expression in transcription and post-transcription levels.

In this study, we profiled proteins interacting with *Gcg* and *Akh* mRNA by RNA affinity pulldown assay and mass spectrometry. We identified numerous proteins, which interacted with *Gcg* and *Akh* mRNA from Drosophila Schneider 2 (S2) and mouse 3T3-L1 cell lysates. Their interactomes revealed RNA-binding proteins, carboxylase, ribosomal protein, and other regulatory proteins. These findings contribute to clarify regulatory mechanisms of *Gcg* and *Akh* decay, translation, and localization via interaction with *Gcg* and *Akh* mRNA.

MATERIALS AND METHODS

1. Culture of mouse 3T3-L1 and Drosophila S2 cells

3T3-L1 cell was obtained from ATCC (ATCC® CL-173™) and cultured in DMEM supplemented with 10% fetal bovine serum (FBS) and penicillin/streptomycin. S2 cell was obtained from ATCC (Schneider's Drosophila Line 2 [D. Mel. (2), SL2]) and cultured in Schneider's Drosophila medium supplemented with 10% FBS and penicillin/streptomycin. The cells were grown in suspension culture at 25℃ without CO_2.

2. mRNA pull down using anti-sense DNA oligo

mRNA pull down using anti-sense DNA oligo was performed as described previously.[23] The biotinylated DNA ologos against mouse *Gcg* mRNA and Drosophila *Akh* mRNA were designed and synthesized in IDT (**Supplementary Table 1**). 3T3-L1 and S2 cell lysates were prepared using protein extraction buffer containing 200 mM Tris-HCl pH 7.5, 100 mM KCl, 5mM MgCl$_2$, 0.5% NP-40 (1 mg per sample), incubated with 1 μg of three different anti-sense DNA oligos with or without biotin label for 4 hours at 4°C. Complexes containing *Gcg* and *Akh* mRNAs were isolated with streptavidin-coupled Sepahrose beads (GE Healthcare, Chicago, IL, USA). The proteins present in the pull-down material were profiled by mass spectrometry and the RNA presents were analyzed by reverse transcription-quantitative polymerase chain reaction (RT-qPCR).

3. Mass spectrometry for protein identification

Gcg and *Akh* mRNA pull down materials were analyzed with mass spectrometry. The proteins were subjected into SDS-polyacrylamide gel electrophoresis (SDS-PAGE) and stained with Coomassie Brilliant Blue. The gel bands were washed with 50 mM ammonium bicarbonate for 10 minutes. Next, the plugs were de-stained using 25 mM ammonium bicarbonate in 50% acetonitrile for 15 minutes, repeated twice. The bands were then reduced with DTT (Sigma-Aldrich, St. Louis, MO, USA) and alkylated using 55 mM Iodoacetamide (Sigma-Aldrich). The gel plugs were then washed with 50 mM ammonium bicarbonate for 10 minutes. The plugs were dehydrated with 100% acetonitrile for 15 minutes and dried in a speedvac. Each gel plug was covered with 100 ng of Proteomics Grade Trypsin (Sigma-Aldrich) and incubated at 37°C overnight. The supernatant was collected in a clean dry Eppendorf tube. Peptides were further extracted with one wash of 25 mM ammonium bicarbonate for 20 minutes and three washes of 5% formic acid, 50% acetonitrile for 20 minutes each. The supernatant was collected after each wash then dried down in a speedvac to ≤1 μL. Samples were reconstituted in 7 μL of mobile phase A (95% water, 5% acetonitrile, and 0.2% formic acid) and placed in auto-sampler vials.

Peptides were separated and analyzed on an EASY nLC 1200 System (Thermo Fisher Scientific, Waltham, MA, USA) in-line with the Orbitrap Fusion Lumos Tribrid Mass Spectrometer (Thermo Fisher Scientific) with instrument control software v. 4.2.28.14. Two μg of tryptic peptides were pressure loaded onto-C18 reversed phase column (Acclaim PepMap RSLC, 75 μm × 50 cm (C18, 2 μm, 100 Å) Thermo Fisher Scientific cat. #164536) using a gradient of 5% to 40% B in 180 minutes (solvent A: 5% acetonitrile/0.1% formic acid; solvent B: 80% acetonitrile/0.1% formic acid) at a flow rate of 300 nL/min.

Mass spectra were acquired in data-dependent mode with a high resolution (60,000) FTMS survey scan, mass range of m/z 375-1500, followed by tandem mass spectra (MS/MS) of the most intense precursors with a cycle time of 3 seconds. The automatic gain control target value was 4.0e5 for the survey MS scan. HCD fragmentation was performed with a precursor isolation window of 1.6 m/z, a maximum injection time of 50 ms, and HCD collision energy of 35%. Monoisotopic-precursor selection was set to "peptide". Precursors within 10 ppm mass tolerance were dynamically excluded from resequencing for 15 seconds. Advanced peak determination was not enabled. Precursor ions with charge states that were undetermined, 1, or >5 were excluded. For protein identification and quantification, the LC-MS/MS data were searched using the MaxQuant (MQ) platform and the protein intensities were normalized using the label free quantification (LFQ) algorithm.[24-26] Data were searched against a *Drosophila melanogaster* or Mus musculus SwissProt reviewed database (August 2020)

and a database of common contaminants. The false discovery rate (FDR), determined using a reversed database strategy, was set at 1% at the protein and peptide level. Fully tryptic peptides with a minimum of 7 residues were required including cleavage between lysine and proline. Two missed cleavages were permitted. The "Label Free Quantitation" (LFQ) feature was used with "Match between runs" enabled for those features that had spectra in at least one of the runs. The "stabilize large ratios" feature was enabled, and "fast LFQ" was disabled. A 4.5 ppm mass tolerance was used. A minimum ratio counts of 2 was required for quantification with at least one unique peptide. Parameters included static modification of cysteine with carbamidomethyl and variable protein N-terminal acetylation and oxidation of methionine. The protein groups text files from the MQ search results were processed in Perseus.[27] Protein groups were filtered to remove those only identified by a modified peptide, matches to the reversed database, and potential contaminants. The normalized LFQ intensities for each biological replicate were log2 transformed.

4. RT-qPCR

RT-qPCR was performed as described previously.[28] Acidic phenol (Ambion) was used to extract RNA from pull down materials. Reverse transcription was performed using random nonamers and reverse transcriptase (Maxima, Thermo Fisher Scientific) followed by qPCR using gene-specific primers (**Supplementary Table 1**) and SYBR green master mix (Kapa Biosystems, Wilmington, MA, USA) under an Applied Biosystems 7300 instrument. Primers against *GAPDH* or *RP49* mRNA were utilized to normalize total amount of RNAs

5. Protein-protein interaction network analysis

Protein-protein interactions were sourced from BioGRID, build 4.3.194.[29] Gene Ontology (GO) analysis utilized GOrilla software.[30] GO term analysis of mass spectrometry hits was performed using all *D. melanogaster* protein coding genes as a background control. Homolog information was extracted from BioMart database within Ensembl.org, release 103.[31] Specifically, "one2one" homologs were used to build the network of hits for homolog networks. For the comparison looking for enrichment compared to all polyA mRNA-binding proteins, the hit list[32] was used as the background control list. Networks were initially created using R software to select the appropriate protein-protein interactions from hit proteins, homologs, and BioGRID data. Output tables were uploaded into Cytoscape 3.8.0 to create visual figures.[33]

6. Protein and RNA purifications from skeletal muscle of young and old mice

"Young" (3-month-old) and "Old" (24-month-old) mouse tibialis anterior muscle were isolated (approved by KRIBB-AEC-16143), homogenized, and lysed with a buffer containing 20 mM HEPES (pH 7.2), 150 mM NaCl, 0.5% Triton X-100, 0.1 mM Na_3VO_4, 1 mM NaF, 1 mM 4-(2-aminoethyl)-benzene sulfonyl fluoride hydrochloride, and 5 mg/mL aprotinin (Sigma-Aldrich).[34] The lysates were centrifuged at 15,000×g for 20 minutes at 4°C, and the supernatants were subjected to SDS-PAGE or acidic phenol extraction for RNA purification followed by immunoblot analysis.

7. Western blot analysis

Cell lysates or pull-down materials were separated by SDS-PAGE and transferred onto nitrocellulose membranes (iBlot Stack; Invitrogen, Waltham, MA, USA). Primary antibodies recognize Plekha7 (GTX131146; GeneTex, Irvine, CA, USA), Vimentin (sc-6260; Santa Cruz Biotechnology, Dallas, TX, USA), Pyruvate Carboxylase B (sc-365673), SRP54 (sc-393855), Plectin (sc-33649) and HSP70 (sc-7298). The horseradish peroxidase-conjugated secondary antibodies were from GE Healthcare.

RESULTS

1. *Akh* mRNA pull down enriches various proteins from Drosophila S2 cells

In order to profile proteins interacting with *D. melanogaster Akh* mRNA, we performed *Akh* mRNA pull down assay followed by mass spectrometry. First, we grew Drosophila S2 cells, extracted lysates using a buffer containing a mild detergent (0.5% NP-40), and then incubated them with biotinylated DNA oligos complementary to *Akh* mRNA (**Fig. 1A**). As a negative control, we utilized the same anti-sense DNA oligos without biotin label. Streptavidin-conjugated sepharose beads were utilized to pull down a complex containing *Akh* mRNA bound to biotinylated anti-sense DNA oligos.

The resulting pellets were subjected either to RNA purification for RT-qPCR (**Fig. 1B**) or SDS-PAGE followed by Coomassie blue staining (**Fig. 1B**). The protein staining revealed enrichment of proteins around 75 kDa, 20 kDa, and 15 kDa, respectively. We also cut the corresponding lanes, extracted/digested proteins from each lane using Trypsin, and then profiled them using mass spectrometry. Our Mass Spectrum revealed that there are 18 major proteins including RNA helicase (bel and Upf1), mRNA translation elongation factors, heterogeneous nuclear ribonucleoproteins (hnRNPs), canonical RNA-binding proteins (lark, larp, and mod), RNA decay enzyme (Rat1), and ribosomal proteins (**Fig. 1C**). These findings demonstrate that *Akh* mRNA establishes molecular complexes containing RNA-binding proteins and ribosomes.

2. *Akh* mRNA interactome revealed clusters of ribosomes and RNA-binding proteins

GO term analysis of mass spectrometry hits indicated select major functions and processes were enriched for mRNA-binding (**Supplementary Table 2**). As expected, molecular function GO analysis showed that RNA-binding (FDR <1.8E-20), mRNA-binding (FDR <1.1E-7), translation regulator activity (FDR <2.2E-6), translation factor activity with RNA-binding (FDR <1.3E-4) were significantly enriched pathways. Biological process GO analysis showed that cytoplasmic translation (FDR < 1.9E-15), gene expression (FDR <2.6E-14), translation (FDR <4.3E-13), peptide biosynthetic process (FDR <5.1E-13), cellular biosynthetic process (FDR <3.2E-09), biosynthetic process (FDR <1.2E-08), regulation of gene expression (FDR <1.2E-05), regulation of alternative mRNA splicing, via spliceosome (FDR <1.3E-05), RNA processing (FDR <3.1E-05) were also significantly enriched pathways. The small ribosomal subunit was enriched (FDR <5.7E-3) whereas the large ribosomal subunit was not. The nucleolus pathway (FDR <6.6E-3) and ribonucleoprotein complex pathway (3.7E-12) were significant. Thus, we interpret mRNA-binding proteins and the small ribosomal subunit regulates *Akh* mRNA translation in Drosophila S2 cells.

A few unexpected pathways also contained select proteins, which led to marginal pathway enrichment. The mitochondrial proton-transporting ATP synthase complex was significantly enriched (FDR <1.8E-3) due to pull down of blw and ATPsyn-beta. Components of microtubule-mediated segregation of cellular components during mitosis were enriched, including spindle microtubule proteins (FDR <7.7E-6). DNA-binding proteins were enriched, particularly in the mitochondria DNA replication pathway (FDR <2.2E-2). These results are highlighted in a network in **Fig. 2A**. Many *Akh* interactions would be expected from non-specific mRNA-binding proteins. To discriminate pan-mRNA binding proteins to *Akh* mRNA-specific binding networks, a background of known Drosophila polyA mRNA-binding proteins was used (**Supplementary Table 3**).[32] Mitochondrion organization (*p*<7.6E-4)

A

Drosophila
S2 cells

↓ lysis

Akh mRNA
pull down

↓ SDS-PAGE

Coomassie blue
staining

↓ Peptide digestion

Mass spectrometry

↓

Peptide matching

B

Akh mRNA
enrichment

Akh mRNA enrichment
(Relative to *RP49* mRNA)

Non-biotin ASO / Biotin ASO

C

M.W. (kDa): 250, 150, 100, 75, 50, 37, 25, 20, 15, 10

1 2 3 — Non-biotin ASO
1 2 3 — Biotin ASO

D

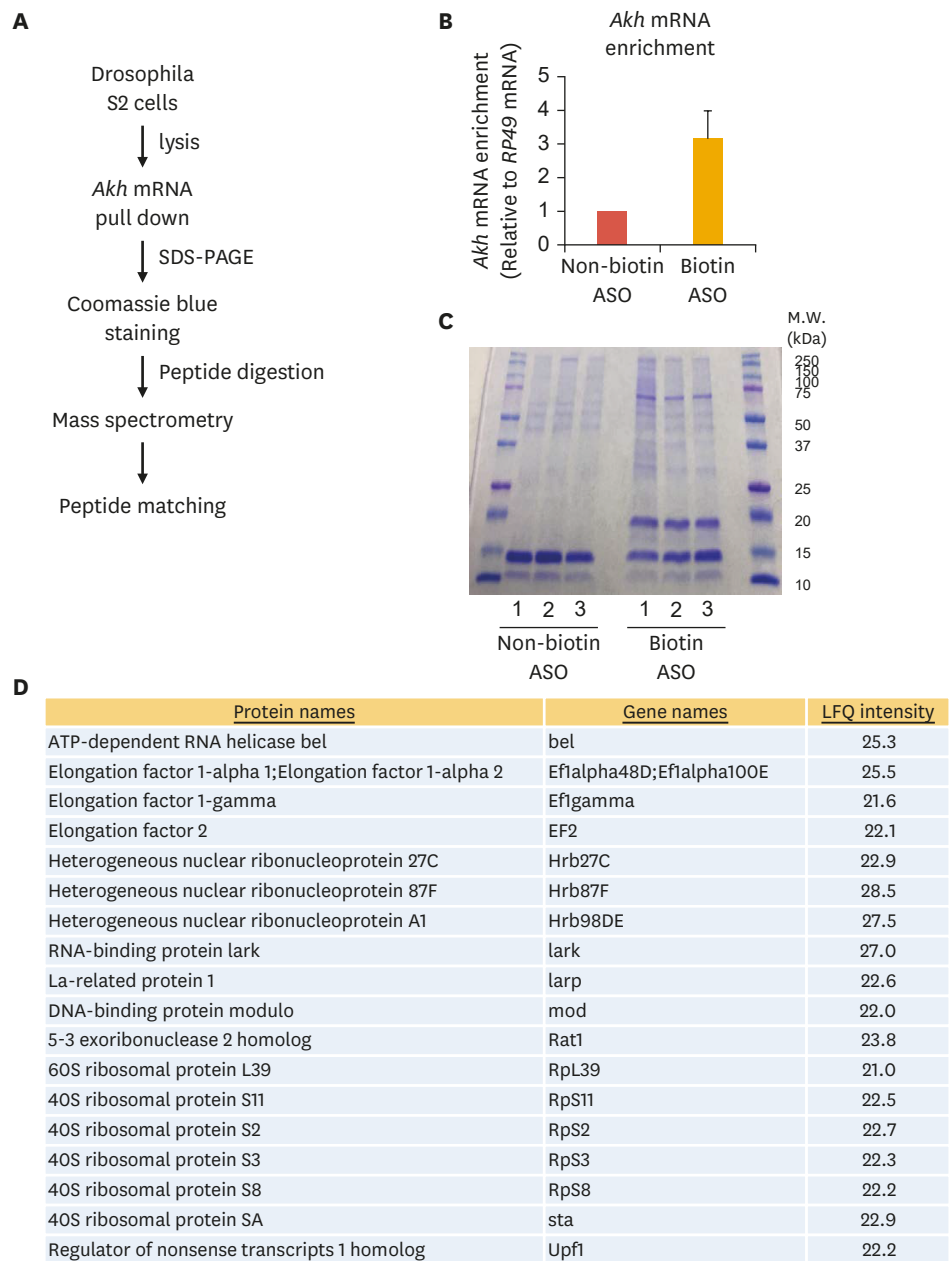| Protein names	Gene names	LFQ intensity
ATP-dependent RNA helicase bel	bel	25.3
Elongation factor 1-alpha 1;Elongation factor 1-alpha 2	Ef1alpha48D;Ef1alpha100E	25.5
Elongation factor 1-gamma	Ef1gamma	21.6
Elongation factor 2	EF2	22.1
Heterogeneous nuclear ribonucleoprotein 27C	Hrb27C	22.9
Heterogeneous nuclear ribonucleoprotein 87F	Hrb87F	28.5
Heterogeneous nuclear ribonucleoprotein A1	Hrb98DE	27.5
RNA-binding protein lark	lark	27.0
La-related protein 1	larp	22.6
DNA-binding protein modulo	mod	22.0
5-3 exoribonuclease 2 homolog	Rat1	23.8
60S ribosomal protein L39	RpL39	21.0
40S ribosomal protein S11	RpS11	22.5
40S ribosomal protein S2	RpS2	22.7
40S ribosomal protein S3	RpS3	22.3
40S ribosomal protein S8	RpS8	22.2
40S ribosomal protein SA	sta	22.9
Regulator of nonsense transcripts 1 homolog	Upf1	22.2

Fig. 1. Identification of *Akh* mRNA-interacting proteins. (A) Experimental scheme of *Akh* mRNA pull-down assay and mass spectrometry from Drosophila S2 cells. (B) *Akh* mRNA enrichment was measured from pull down materials using non-biotin ASO and biotin ASO followed by reverse transcription-quantitative polymerase chain reaction. (C) SDS-PAGE and Coomassie blue staining of proteins from *Akh* mRNA pull down. (D) List of proteins identified from mass spectrometry.
mRNA, messenger RNA; S2, Schneider 2; ASO, antisense oligonucleotide; SDS-PAGE, SDS-polyacrylamide gel electrophoresis; LFQ, label free quantification.

remained nominally enriched when compared to known polyA mRNA-binding proteins, as did microtubule component (FDR <8.6E-9) and DNA binding (FDR <2.4E-5). These results are highlighted in a network in **Fig. 2B**. Taken together, these results indicate DNA binding factors and mitochondria-microtubule protein networks interact with *Akh* mRNA at higher rates than expected by chance.
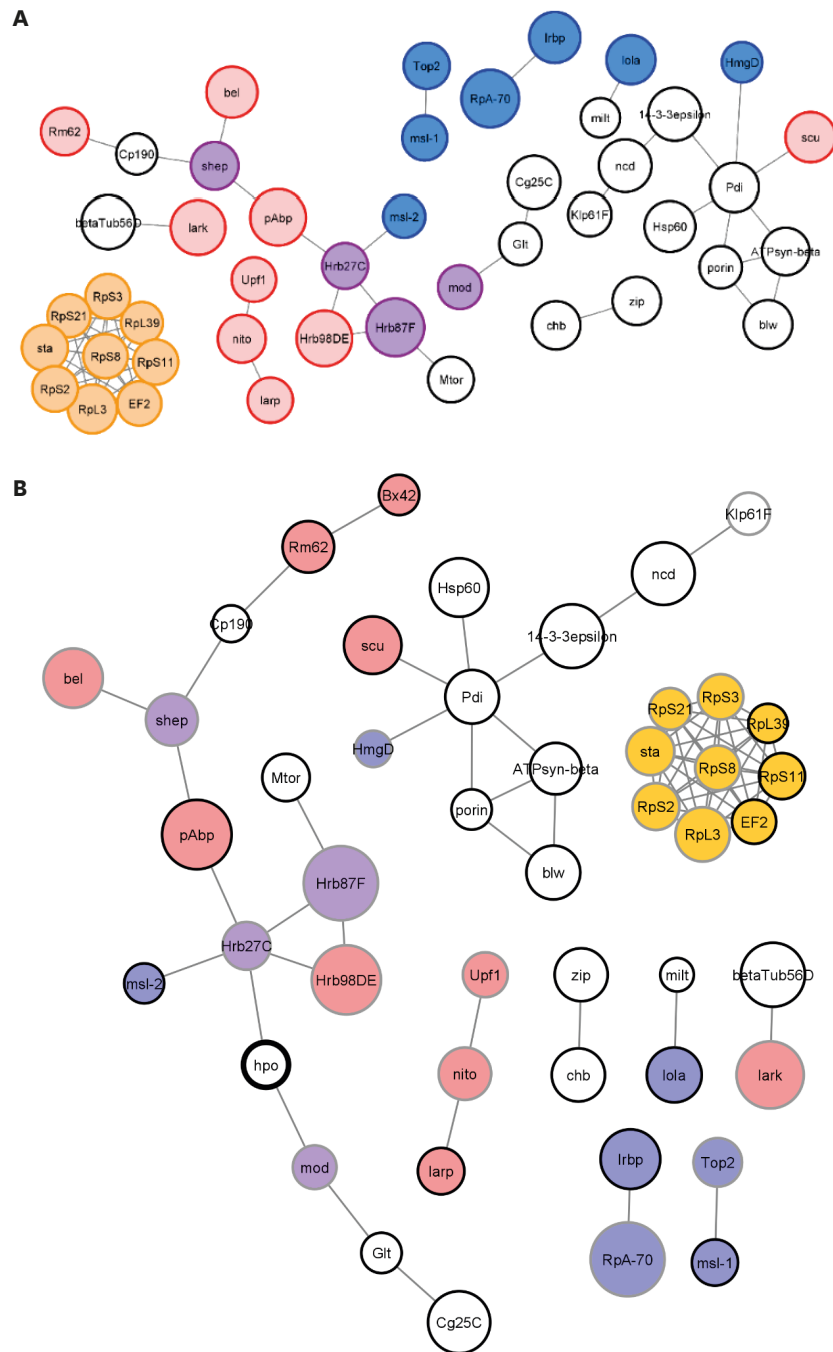
Fig. 2. Protein-protein interaction plot of *Akh* mRNA-interacting proteins. (A) Protein-protein interactions of hits identified in proteomic analysis. Edges are derived from BioGRID. Blue indicates DNA-binding proteins, red indicates RNA-binding proteins, and purple indicates dual RNA/DNA-binding proteins. Orange indicates ribosomal proteins. White fill indicates the other proteins, particularly microtubule-binding proteins and mitochondrial proteins. The circle size is proportional to mass spectrometry signal data. (B) Protein-protein interactions of hits identified in proteomic analysis after normalization with polyA mRNA-binding protein profiles. Edges are derived from BioGRID. Blue indicates DNA-binding proteins, red indicates RNA-binding proteins, and purple indicates dual RNA/DNA-binding proteins. Orange indicates ribosomal proteins. White fill indicates other protein classes, particularly microtubule-binding proteins and mitochondrial proteins. The circle size is proportional to mass spectrometry signal data. Gray node outlines indicate known polyA mRNA-binding proteins in Drosophila, black edges indicate previously unidentified hits. Hpo was manually added and were not a hit in the current proteomic profile.

mRNA, messenger RNA.

A complementary method of analyzing how *Akh* mRNA interacts with mRNA-bound proteins is to determine how *Akh* interactors relate to the overall polyA mRNA interactome. To do this, a network was generated from protein-protein interactions within the polyA mRNA-interactome and *Akh* mRNA-binding proteins were highlighted within the network. This is essentially the reverse of the network building strategy from **Fig. 2B**. As might be expected, the network of all known polyA-binding proteins was much more extensive than the *Akh*-specific binding protein network (**Fig. 3**). Nonetheless, the *Akh* mRNA-binding proteins were spread evenly throughout the pan-polyA binding network. Taken together with the networks in **Fig. 2**, these results indicate *Akh* mRNA is not handled as an "average" mRNA transcript from Drosophila S2 cells.

3. Mouse *Gcg* mRNA interactome revealed mRNA-binding protein, carboxylase and lipid metabolism related enzyme

To profile proteins interacting with the AKH homolog in mouse, *Gcg* mRNA, we performed *Gcg* mRNA pull down assay and mass spectrometry. 3T3-L1 lysates were incubated with biotinylated or non-biotinylated DNA oligos complementary to *Gcg* mRNA (**Fig. 4A**). Streptavidin-conjugated sepharose beads enabled us to pull down a complex containing *Gcg* mRNA bound to the biotinylated DNA oligos. The pull-down materials were subjected either to RNA purification for RT-qPCR (**Fig. 4B**) or SDS-PAGE followed by mass spectrometry (**Fig. 4C**). Our Mass spectrum revealed that there are 34 protein hits including mRNA-binding protein (SERBP1), zinc finger protein (ZFP28), carboxylases (Acetyl-CoA carboxylase, Methylcrotonoyl-CoA carboxylase and Pyruvate Carboxylase), lipase (diacylglycerol lipase beta), histone proteins, signal recognition particle 54 (SRP54), cytoskeletal protein (Plectin, Plekha7, and Vimentin) and CYP2C44 (**Fig. 4C**). We verified that Plekha7 interacts with *Gcg* mRNA using western blot analysis (**Fig. 4D**). These findings demonstrate that *Gcg* mRNA establishes molecular complexes containing RNA-binding proteins, carboxylase, or lipid metabolism related enzymes.

4. *Gcg* mRNA interactome revealed nucleosomal DNA-binding and protein-DNA complex enrichment

GO term analysis of mass spectrometry hits did not show identical regulation of *Gcg* mRNA translation as might be expected from the *Akh* mRNA interactome. Few molecular functions, biological processes and cellular components of GO term analysis were significant FDR (**Supplementary Table 4**). Nucleosomal DNA-binding enriched nucleosomal DNA-binding (FDR <7.3E-3), nucleosome (FDR <7.1E-6) and DNA packaging complex (FDR <1.1E-5) were significantly enriched pathways. However, we could not find enriched GO term data of mRNA regulation, carboxylase or lipid metabolism related enzyme as we observed from *Akh* mRNA interactome. Both the *Gcg* and *Akh* datasets unexpectedly contained enrichment of DNA binding factors, suggesting these proteins may have additional non-canonical functions regulating mRNA as well.

5. Network plot of *Gcg* mRNA-interacting proteins revealed cluster of histone proteins

A network plot of *Gcg* mRNA interactions revealed that the most of the identified proteins clusters are in histone family proteins (**Fig. 5A**). They are connected each other with histone proteins both directly and indirectly, which are functionally connected with packaging DNA into chromatin in nucleus.[35] GO analysis also revealed that nucleosomal DNA-binding (FDR <7.3E-3), nucleosome (FDR <7.1E-6) and DNA packaging complex (FDR <1.1E-5) were significantly enriched pathways. Another cluster centered with ryanodine receptor 2 or
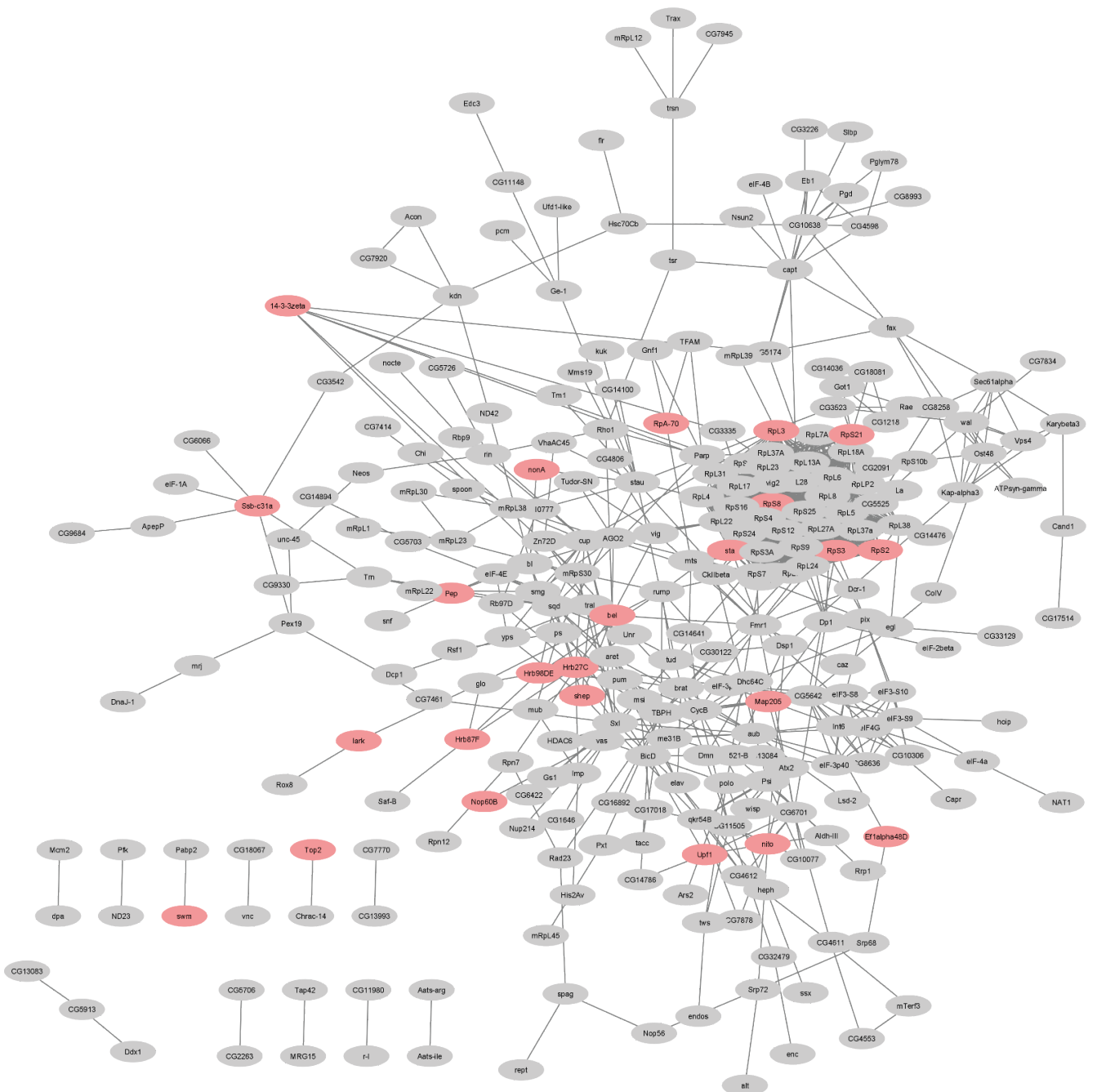
Fig. 3. Network plot of the polyA mRNA-binding proteome for *Drosophila melanogaster* tissues. Red nodes indicate *Akh* mRNA-interacting proteome hits and grey nodes indicate all other previously identified polyA mRNA-binding proteins. Interactions are derived from *D. melanogaster* BioGRID protein-protein interactions. mRNA, messenger RNA.

ZFP28 were not connected with histone proteins in first-neighbor network analysis (**Fig. 5A**). Therefore, the network plot may be interpreted to show that most of *Gcg* mRNA-interacting proteins are possibly located in nucleus and involved in chromatin regulation.

6. Level of *Gcg* mRNA correlates with levels of *Gcg* mRNA-interacting proteins in aged mouse skeletal muscle

In order to connect our findings in *Gcg* mRNA-interactome with biological processes, we first
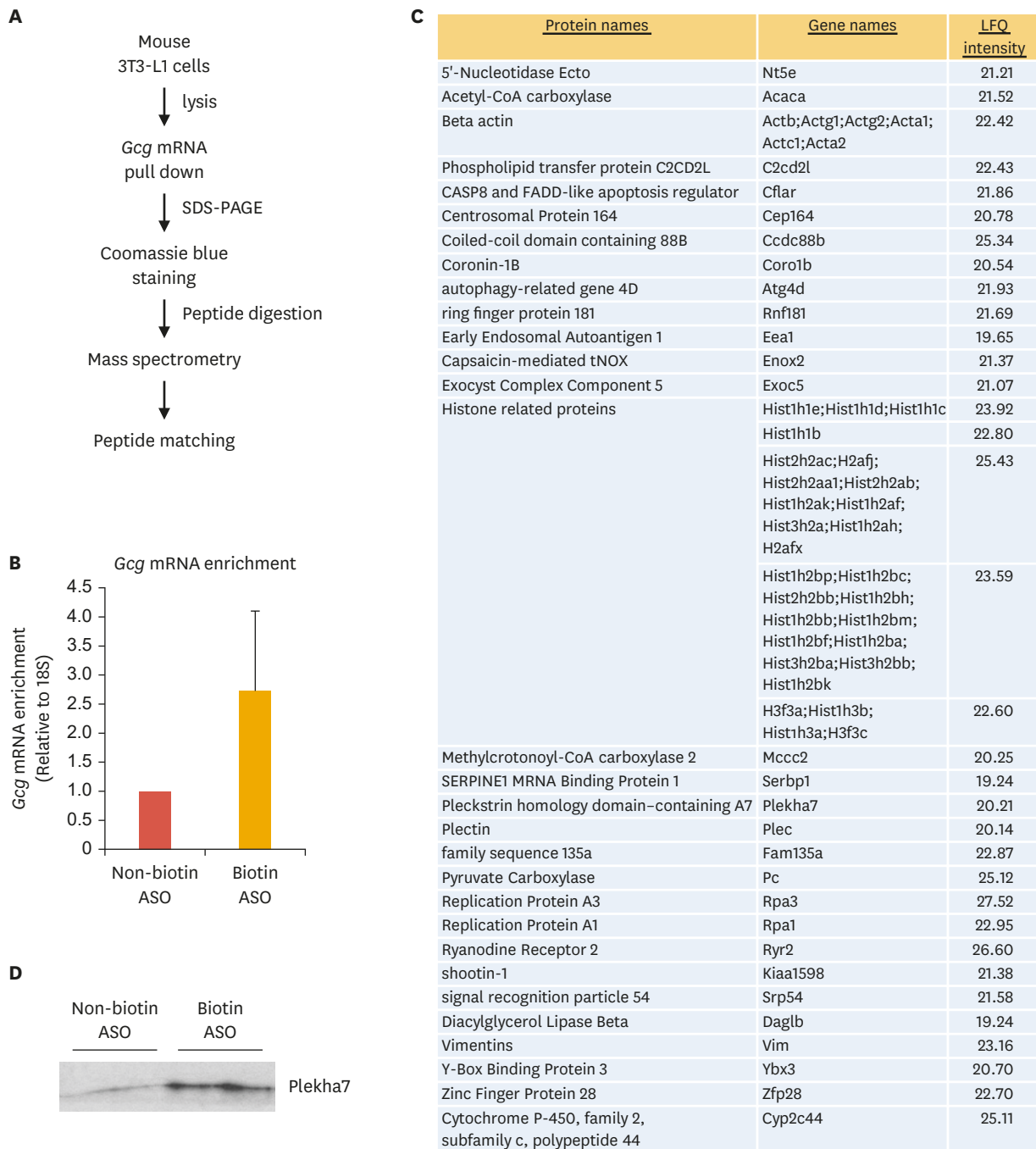
A

Mouse
3T3-L1 cells

↓ lysis

Gcg mRNA
pull down

↓ SDS-PAGE

Coomassie blue
staining

↓ Peptide digestion

Mass spectrometry

↓

Peptide matching

B

Gcg mRNA enrichment

C

Protein names	Gene names	LFQ intensity
5'-Nucleotidase Ecto	Nt5e	21.21
Acetyl-CoA carboxylase	Acaca	21.52
Beta actin	Actb;Actg1;Actg2;Acta1;Actc1;Acta2	22.42
Phospholipid transfer protein C2CD2L	C2cd2l	22.43
CASP8 and FADD-like apoptosis regulator	Cflar	21.86
Centrosomal Protein 164	Cep164	20.78
Coiled-coil domain containing 88B	Ccdc88b	25.34
Coronin-1B	Coro1b	20.54
autophagy-related gene 4D	Atg4d	21.93
ring finger protein 181	Rnf181	21.69
Early Endosomal Autoantigen 1	Eea1	19.65
Capsaicin-mediated tNOX	Enox2	21.37
Exocyst Complex Component 5	Exoc5	21.07
Histone related proteins	Hist1h1e;Hist1h1d;Hist1h1c	23.92
	Hist1h1b	22.80
	Hist2h2ac;H2afj;Hist2h2aa1;Hist2h2ab;Hist1h2ak;Hist1h2af;Hist3h2a;Hist1h2ah;H2afx	25.43
	Hist1h2bp;Hist1h2bc;Hist2h2bb;Hist1h2bh;Hist1h2bb;Hist1h2bm;Hist1h2bf;Hist1h2ba;Hist3h2ba;Hist3h2bb;Hist1h2bk	23.59
	H3f3a;Hist1h3b;Hist1h3a;H3f3c	22.60
Methylcrotonoyl-CoA carboxylase 2	Mccc2	20.25
SERPINE1 MRNA Binding Protein 1	Serbp1	19.24
Pleckstrin homology domain–containing A7	Plekha7	20.21
Plectin	Plec	20.14
family sequence 135a	Fam135a	22.87
Pyruvate Carboxylase	Pc	25.12
Replication Protein A3	Rpa3	27.52
Replication Protein A1	Rpa1	22.95
Ryanodine Receptor 2	Ryr2	26.60
shootin-1	Kiaa1598	21.38
signal recognition particle 54	Srp54	21.58
Diacylglycerol Lipase Beta	Daglb	19.24
Vimentins	Vim	23.16
Y-Box Binding Protein 3	Ybx3	20.70
Zinc Finger Protein 28	Zfp28	22.70
Cytochrome P-450, family 2, subfamily c, polypeptide 44	Cyp2c44	25.11

D

Non-biotin ASO | Biotin ASO

Plekha7

Fig. 4. Investigation of *Gcg* mRNA-interacting proteins. (A) Experimental scheme of *Gcg* mRNA pull-down assay and mass spectrometry from mouse 3T3-L1 cells. (B) *Gcg* mRNA enrichment was measured from pull down materials using non-biotin ASO and biotin ASO followed by reverse transcription-quantitative polymerase chain reaction. (C) List of *Gcg* mRNA-interacting proteins identified from mass spectrometry. (D) Western blot analysis of Plekha7 from pull down materials using non-biotin ASO and biotin-ASO.
mRNA, messenger RNA; SDS-PAGE, SDS-polyacrylamide gel electrophoresis; ASO, antisense oligonucleotide; LFQ, label free quantification.

compared levels of *Gcg* mRNA in lysates of skeletal muscle isolated from young (3 months) and old (24 months) mice. Our RT-qPCR analysis revealed that levels of *Gcg*, *Dlk1*, and *Pparg* mRNAs are elevated in old muscle tissues while *Fabp4* mRNA did not fluctuate (**Fig. 5B**). Western blot analysis of *Gcg* mRNA-interacting proteins showed that levels of Plekha7, Pyruvate Carboxylase
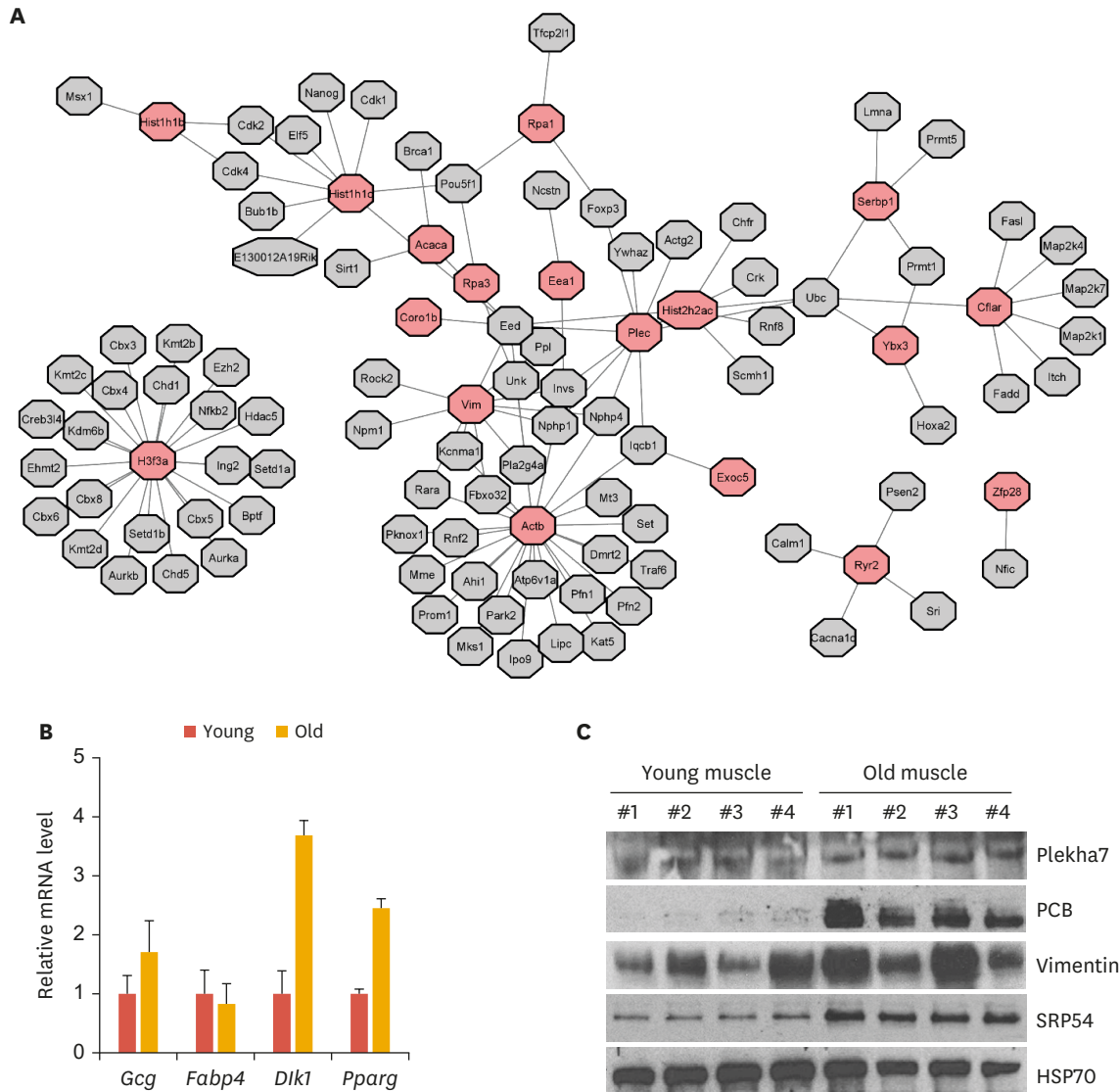
Fig. 5. Network plot of *Gcg* mRNA-interacting proteins identified from mass spectrometry. (A) Red nodes indicate *Gcg* mRNA-interacting proteome hits and grey nodes indicate known interacting proteins, which were not identified from mass spectrometry. Interactions are derived from *Mus musculus* BioGRID protein-protein interactions. (B) Reverse transcription-quantitative polymerase chain reaction analysis of *Gcg*, *Pparg*, *Fabp4*, and *Dlk1* mRNAs purified from skeletal muscle of young (3 month) and old (24 month) mice. (C) Western blot analysis of Plekha7, PCB, Vimentin, SRP54, and HSP70 using young and old mice muscle tissue. mRNA, messenger RNA; PCB, Pyruvate Carboxylase B.

B, Vimentin, and SRP54 increased while the level of loading control HSP70 did not change as a loading control (**Fig. 5C**). These results implicate accumulation of *Gcg* mRNA in old skeletal muscle may originate from overexpression of *Gcg* mRNA-interacting proteins.

DISCUSSION

Glucagon and insulin are key hormones regulating lipid metabolism and glucose levels in blood.[36] Dysregulation of these hormones induces obesity, hyperlipidemia, diabetes and even cancers.[37-39] Although there is much published research regarding transcriptional regulation of AKH, DILP, glucagon and insulin expression,[18,40] post-transcriptional regulation of *Akh*, and Gcg mRNA

translation remains unclear.[18] In this study, we found that numerous proteins interact with *Akh* and *Gcg* mRNA in Drosophila S2 and mouse 3T3-L1 cells. (**Figs. 1** and **4**). *Akh* mRNA interactomes revealed clusters of ribosomes and RNA-binding proteins (**Figs. 2** and **3**) whereas mouse *Gcg* mRNA interactomes revealed RNA-binding protein, carboxylase and lipid metabolism.

Eighteen major proteins include RNA helicase (bel and Upf1), mRNA translation elongation factors, hnRNPs, RNA-binding proteins (lark, larp and mod), RNA decay enzyme Rat1 and ribosomal proteins (**Fig. 1D**). RNA-binding proteins lark, larp and mod were reported to activate post-transcriptional regulation of translation.[28,41,42] Therefore, *Akh* mRNA post-transcriptional regulation of translation is possible to relate with RNA-binding proteins of lark, larp and mod. RNA-binding proteins larp6 activates mRNA translation via recruitment of ATP-dependent RNA helicase A,[43] which might function similarly with RNA helicase bel and Upf1 on *Akh* mRNA. On the other hand, RNA decay enzyme Rat1may degrade *Akh* mRNA via 5′ to 3′.[44] We expected RNA-binding proteins of lark, larp and mod and RNA decay enzyme Rat1 could function in regulation of *Akh* mRNA decay and translation, respectively.[28,41,42,44] Detailed information is provided in the schematic in **Fig. 6A**.

GO term analysis also supported regulation of *Akh* mRNA translation. Molecular function of GO term analysis showed their proteins highly related with mRNA-binding and translation (**Supplementary Table 2**). Biological process of GO term analysis also showed their proteins highly related with translation and biosynthetic process (**Supplementary Table 2**). In addition, cellular component of GO term analysis highlighted that *Akh* mRNA was enriched with both small and large ribosomal subunits (**Supplementary Table 2**). The cytosolic ribosome pathway was enriched largely due to binding of ribonucleoproteins and small and large ribosomal subunits (**Fig. 1D**, **Supplementary Tables 2** and **3**). We interpret that *Akh* mRNA translation are under regulation with various proteins in cytosolic ribosome. Further study is needed for clarifying the interaction between *Akh* mRNA and our identified interacting proteins. However, our study showed the possibility of *Akh* mRNA interaction and regulation with 18 proteins.

Thirty-four major proteins include mRNA-binding protein (SERBP1), ZFP28, carboxylase (Acetyl-CoA carboxylase, Methylcrotonoyl-CoA carboxylase and Pyruvate Carboxylase), lipase (diacylglycerol lipase beta), histone proteins, SRP54, cytoskeletal protein (Plectin, Plekha7, and Vimentin) and Cyp2c44. We also found mRNA-binding protein of SERBP1 involved in gene expression regulation.[45] It is reported that SERBP1 binds with *CtIP* mRNA and regulates polysome-associated *CtIP* mRNA translation.[46] As a 54 kDa subunit protein of signal recognition protein, SRP54 has a methionine-rich RNA-binding domain directly interacting with 4.5S RNA,[47] which is conserved in mouse and human. Vimentin also co-precipitates with a long noncoding RNA, BC088259,[48] mouse mu opioid receptor mRNA,[49] and collagen mRNAs,[50] implicating its direct interaction with RNAs. In addition, we verified that Plekha7 interacts with *Gcg* mRNA using RNA pull down and western blot analysis (**Fig. 4D**). Plekha7 was also implicated in direct or indirect association with mature miRNAs.[51,52] Interaction of SERBP1, SRP54, Plekha7 and Vimentin with *Gcg* mRNA require further study to define biochemical regulatory mechanisms. A previous study reported proglucagon mRNA-binding protein of HuD was not found in our study possibly due to low expression of HuD in undifferentiated 3T3-L1 cells.[22] More details are provided in the schematic in **Fig. 6B**.

In contrast to *Akh* mRNA-interacting proteins GO analysis, *Gcg* GO analysis did not support specific regulation of *Gcg* mRNA translation in undifferentiated 3T3-L1 cells (**Fig. 5**, **Supplementary Table 4**). The mass spectrometry data enriched nucleosome DNA-binding
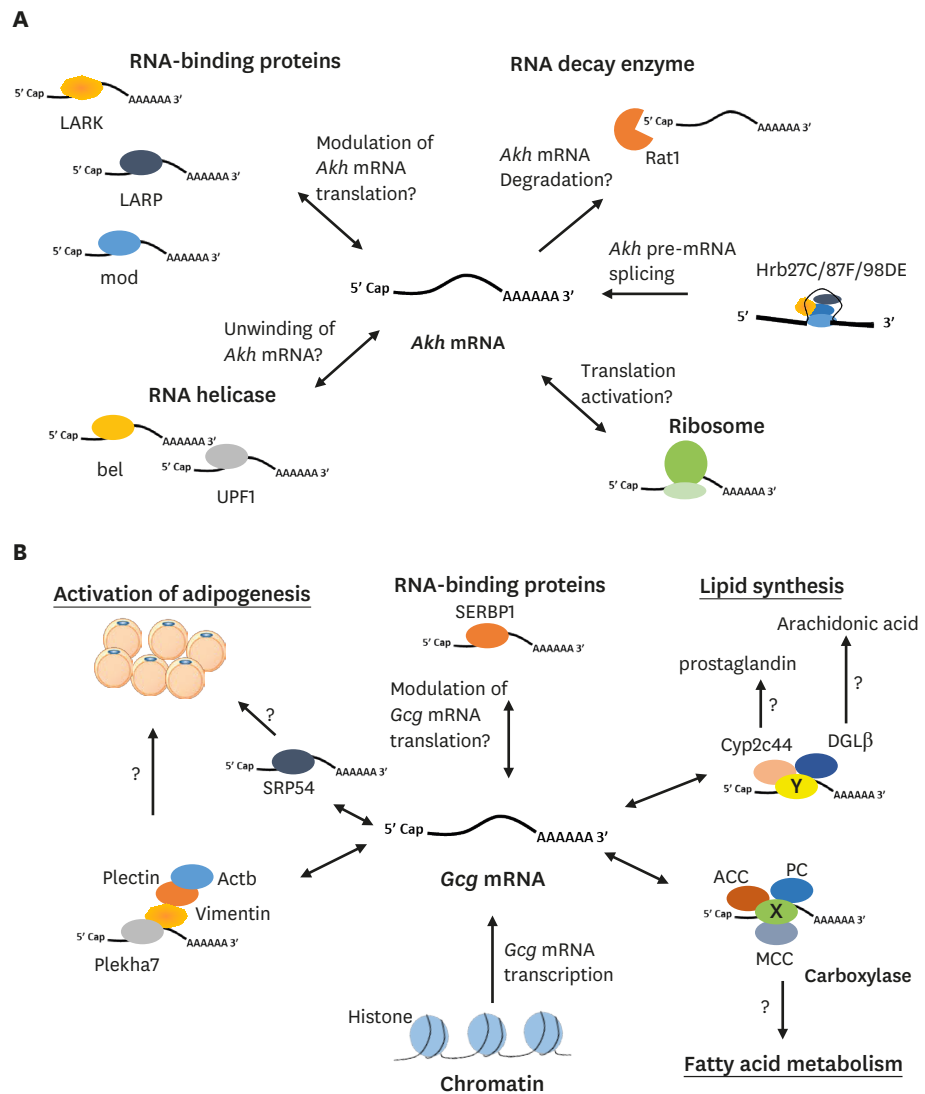
Fig. 6. Anticipated schematic of *Akh* and *Gcg* mRNA interactomes. (A) Schematic of *Akh* mRNA-interacting proteins such as RNA-binding proteins (LARK, LARP, and mod), RNA-decay enzyme (Rat1), snRNPs (Hrb27c, 87F, and 98DE), ribosomal proteins and RNA helicases (bel and UPF1) in complex with *Akh* mRNA. (B) Schematic of *Gcg* mRNA-interacting proteins such as RNA-binding protein (SERBP1), cytoskeletal proteins (Plekha7, Plectin, Vimentin, and β-Actin), SRP54, histones, carboxylase (MCC, ACC and PC) and lipid metabolic enzyme (Cyp2c44 and DGLβ). SERBP1, SRP54, Plekha7, and Vimentin could be RNA-binding proteins for unidentified RNA-binding protein X (green) and Y (yellow).
mRNA, messenger RNA; SRP54, signal recognition protein 54.

because of histone family proteins (**Supplementary Table 4**). We interpret the results both *Gcg* precursor and mature mRNAs were pull down with chromatin undergoing active transcription but still processing precursor mRNAs. Furthermore, we attempted *Gcg* mRNA pull down assay using 3T3-L1 cells after differentiation into adipocyte-like cells. However, we did not obtain enough amount of proteins for mass spectrometry from *Gcg* mRNA pull down materials. If this is the case, we can explain why GO analysis didn't show RNA-binding proteins and ribosomes under active translation.

Interestingly, Acetyl-CoA carboxylase, Pyruvate Carboxylase and Methylcrotonoyl-CoA carboxylase interacted with *Gcg* mRNA (**Fig. 4C**). Downstream signaling of glucagon and its

receptor inactivates Acetyl-CoA carboxylase and Acetyl-CoA carboxylase mRNA transcription as a result of blocking synthesis of fatty acid.[2,53] Methylcrotonoyl-CoA carboxylase also relates synthesis of fatty acid with Acetyl-CoA carboxylase.[54] Contrary to the previous research indicating that two enzymes in this reaction are inhibited by glucagon[2,53] and interact with *Gcg* mRNA, we speculate that these enzymes might be involved in inhibition of *Gcg* mRNA translation or activation of *Gcg* mRNA decay. Although there are no studies showing that these carboxylases bind RNA directly, they may interact with *Gcg* mRNA via other RNA-binding proteins. On the other hand, Pyruvate Carboxylase relates glucose synthesis by converting pyruvate to oxaloacetate.[55] Glucagon affects flux of Pyruvate Carboxylase for carboxylation of pyruvate.[56] Pyruvate Carboxylase might be involved in activation of *Gcg* mRNA translation or inhibition of *Gcg* mRNA decay. Interaction of Acetyl-CoA carboxylase, Pyruvate Carboxylase and Methylcrotonoyl-CoA carboxylase with *Gcg* mRNA need further investigation to explore post-transcriptional regulation of *Gcg* mRNA.

Diacylglycerol lipase beta and Cyp2c44 interacted with *Gcg* mRNA in this study. They relate with synthesis of arachidonic acid and prostaglandin, respectively.[57,58] Arachidonic acid and prostaglandin are key factors of lipid metabolism.[59,60] We speculate that lipid metabolic pathways could be related to translation or decay of *Gcg* mRNA. Interaction diacylglycerol lipase beta and Cyp2c44 with *Gcg* mRNA are not known previously, but arachidonic acid and prostaglandin pathways are involved in glucagon-mediated lipolysis.[61] Further studies on the relationship between lipid metabolism and glucagon are needed in terms of *Gcg* mRNA decay and translation.

Our findings in young and old skeletal muscle implicate relevance of adipogenesis and skeletal muscle biology. Glucagon modulates proliferation and differentiation of human adipose precursors cells,[62] which might happen similarly in intermuscular adipose tissues.[63] Cytoskeletal proteins such as Vimentin, Plectin, and Plekha7 are also involved in lipogenesis,[64] lipid droplet assembly[65] and direct binding with phosphatidylinositol lipids,[66] respectively. Molecular mechanisms of how *Gcg* mRNA-interacting proteins stabilizes *Gcg* mRNA in skeletal muscle should be investigated thoroughly.

In summary, we profiled various proteins interacting with *Gcg* and *Akh* mRNA. These newly identified proteins could be the start points for identifying the post-transcription regulatory mechanisms of *Gcg* and *Akh* mRNA.

SUPPLEMENTARY MATERIALS

Supplementary Table 1
Sequences of primers used in this study

Click here to view

Supplementary Table 2

Drosophila melanogaster gene ontology analysis

Click here to view

Supplementary Table 3

Drosophila melanogaster gene ontology analysis normalized with polyA mRNA-binding proteome

Click here to view

Supplementary Table 4

Mus musculus gene ontology analysis

Click here to view

REFERENCES

1. Arrese EL, Mirza S, Rivera L, Howard AD, Chetty PS, Soulages JL. Expression of lipid storage droplet protein-1 may define the role of AKH as a lipid mobilizing hormone in Manduca sexta. Insect Biochem Mol Biol 2008;38:993-1000.
   PUBMED | CROSSREF

2. Galsgaard KD, Pedersen J, Knop FK, Holst JJ, Wewer Albrechtsen NJ. Glucagon receptor signaling and lipid metabolism. Front Physiol 2019;10:413.
   PUBMED | CROSSREF

3. Heimberg M, Weinstein I, Kohout M. The effects of glucagon, dibutyryl cyclic adenosine 3′,5′-monophosphate, and concentration of free fatty acid on hepatic lipid metabolism. J Biol Chem 1969;244:5131-5139.
   PUBMED | CROSSREF

4. von Meyenn F, Porstmann T, Gasser E, Selevsek N, Schmidt A, Aebersold R, et al. Glucagon-induced acetylation of Foxa2 regulates hepatic lipid metabolism. Cell Metab 2013;17:436-447.
   PUBMED | CROSSREF

5. Ziegler R, Eckart K, Law JH. Adipokinetic hormone controls lipid metabolism in adults and carbohydrate metabolism in larvae of Manduca sexta. Peptides 1990;11:1037-1040.
   PUBMED | CROSSREF

6. Rivers DB, Denlinger DL. Venom-induced alterations in fly lipid metabolism and its impact on larval development of the ectoparasitoid Nasonia vitripennis (Walker)(Hymenoptera: Pteromalidae). J Invertebr Pathol 1995;66:104-110.
   CROSSREF

7. Wang S, Liu S, Liu H, Wang J, Zhou S, Jiang RJ, et al. 20-hydroxyecdysone reduces insect food consumption resulting in fat body lipolysis during molting and pupation. J Mol Cell Biol 2010;2:128-138.
   PUBMED | CROSSREF

8. Hossain MS, Liu Y, Zhou S, Li K, Tian L, Li S. 20-Hydroxyecdysone-induced transcriptional activity of FoxO upregulates brummer and acid lipase-1 and promotes lipolysis in Bombyx fat body. Insect Biochem Mol Biol 2013;43:829-838.
   PUBMED | CROSSREF

9. Liljenquist JE, Bomboy JD, Lewis SB, Sinclair-Smith BC, Felts PW, Lacy WW, et al. Effects of glucagon on lipolysis and ketogenesis in normal and diabetic men. J Clin Invest 1974;53:190-197.
   PUBMED | CROSSREF

10. Men TT, Binh TD, Yamaguchi M, Huy NT, Kamei K. Function of lipid storage droplet 1 (Lsd1) in wing development of Drosophila melanogaster. Int J Mol Sci 2016;17:648.
    PUBMED | CROSSREF

11. Zimmermann R, Strauss JG, Haemmerle G, Schoiswohl G, Birner-Gruenberger R, Riederer M, et al. Fat mobilization in adipose tissue is promoted by adipose triglyceride lipase. Science 2004;306:1383-1386.
    PUBMED | CROSSREF

12. Schreiber R, Xie H, Schweiger M. Of mice and men: the physiological role of adipose triglyceride lipase (ATGL). Biochim Biophys Acta Mol Cell Biol Lipids 2019;1864:880-899.
    PUBMED | **CROSSREF**

13. Slavin BG, Ong JM, Kern PA. Hormonal regulation of hormone-sensitive lipase activity and mRNA levels in isolated rat adipocytes. J Lipid Res 1994;35:1535-1541.
    PUBMED | **CROSSREF**

14. Oberer M, Boeszoermenyi A, Nagy HM, Zechner R. Recent insights into the structure and function of comparative gene identification-58. Curr Opin Lipidol 2011;22:149.
    PUBMED | **CROSSREF**

15. Granneman JG, Moore HP, Krishnamoorthy R, Rathod M. Perilipin controls lipolysis by regulating the interactions of AB-hydrolase containing 5 (Abhd5) and adipose triglyceride lipase (Atgl). J Biol Chem 2009;284:34538-34544.
    PUBMED | **CROSSREF**

16. Post S, Liao S, Yamamoto R, Veenstra JA, Nässel DR, Tatar M. Drosophila insulin-like peptide dilp1 increases lifespan and glucagon-like Akh expression epistatic to dilp2. Aging Cell 2019;18:e12863.
    PUBMED | **CROSSREF**

17. Petersen MC, Vatner DF, Shulman GI. Regulation of hepatic glucose metabolism in health and disease. Nat Rev Endocrinol 2017;13:572-587.
    PUBMED | **CROSSREF**

18. Gosmain Y, Cheyssac C, Heddad Masson M, Dibner C, Philippe J. Glucagon gene expression in the endocrine pancreas: the role of the transcription factor Pax6 in α-cell differentiation, glucagon biosynthesis and secretion. Diabetes Obes Metab 2011;13 Suppl 1:31-38.
    PUBMED | **CROSSREF**

19. Gosmain Y, Avril I, Mamin A, Philippe J. Pax-6 and c-Maf functionally interact with the α-cell-specific DNA element G1 *in vivo* to promote glucagon gene expression. J Biol Chem 2007;282:35024-35034.
    PUBMED | **CROSSREF**

20. Gauthier BR, Schwitzgebel VM, Zaiko M, Mamin A, Ritz-Laser B, Philippe J. Hepatic nuclear factor-3 (HNF-3 or Foxa2) regulates glucagon gene transcription by binding to the G1 and G2 promoter elements. Mol Endocrinol 2002;16:170-183.
    PUBMED | **CROSSREF**

21. Kaestner KH, Katz J, Liu Y, Drucker DJ, Schütz G. Inactivation of the winged helix transcription factor HNF3α affects glucose homeostasis and islet glucagon gene expression *in vivo*. Genes Dev 1999;13:495-504.
    PUBMED | **CROSSREF**

22. Ahn S, Tak H, Kang H, Ryu S, Jeong SM, Kim W, et al. The RNA-binding protein, HuD regulates proglucagon biosynthesis in pancreatic α cells. Biochem Biophys Res Commun 2020;530:266-272.
    PUBMED | **CROSSREF**

23. Yoon JH, Abdelmohsen K, Srikantan S, Yang X, Martindale JL, De S, et al. LincRNA-p21 suppresses target mRNA translation. Mol Cell 2012;47:648-655.
    PUBMED | **CROSSREF**

24. Cox J, Mann M. MaxQuant enables high peptide identification rates, individualized p.p.b.-range mass accuracies and proteome-wide protein quantification. Nat Biotechnol 2008;26:1367-1372.
    PUBMED | **CROSSREF**

25. Cox J, Hein MY, Luber CA, Paron I, Nagaraj N, Mann M. Accurate proteome-wide label-free quantification by delayed normalization and maximal peptide ratio extraction, termed MaxLFQ. Mol Cell Proteomics 2014;13:2513-2526.
    PUBMED | **CROSSREF**

26. Tyanova S, Temu T, Cox J. The MaxQuant computational platform for mass spectrometry-based shotgun proteomics. Nat Protoc 2016;11:2301-2319.
    PUBMED | **CROSSREF**

27. Tyanova S, Temu T, Sinitcyn P, Carlson A, Hein MY, Geiger T, et al. The Perseus computational platform for comprehensive analysis of (prote)omics data. Nat Methods 2016;13:731-740.
    PUBMED | **CROSSREF**

28. Lista MJ, Martins RP, Billant O, Contesse MA, Findakly S, Pochard P, et al. Nucleolin directly mediates Epstein-Barr virus immune evasion through binding to G-quadruplexes of EBNA1 mRNA. Nat Commun 2017;8:16043.
    PUBMED | **CROSSREF**

29. Stark C, Breitkreutz BJ, Reguly T, Boucher L, Breitkreutz A, Tyers M. BioGRID: a general repository for interaction datasets. Nucleic Acids Res 2006;34:D535-D539.
    PUBMED | **CROSSREF**

30. Eden E, Navon R, Steinfeld I, Lipson D, Yakhini Z. GOrilla: a tool for discovery and visualization of enriched GO terms in ranked gene lists. BMC Bioinformatics 2009;10:48.
PUBMED | CROSSREF

31. Yates AD, Achuthan P, Akanni W, Allen J, Allen J, Alvarez-Jarreta J, et al. Ensembl 2020. Nucleic Acids Res 2020;48:D682-D688.
PUBMED | CROSSREF

32. Sysoev VO, Fischer B, Frese CK, Gupta I, Krijgsveld J, Hentze MW, et al. Global changes of the RNA-bound proteome during the maternal-to-zygotic transition in Drosophila. Nat Commun 2016;7:12128.
PUBMED | CROSSREF

33. Shannon P, Markiel A, Ozier O, Baliga NS, Wang JT, Ramage D, et al. Cytoscape: a software environment for integrated models of biomolecular interaction networks. Genome Res 2003;13:2498-2504.
PUBMED | CROSSREF

34. Lee SM, Lee SH, Jung Y, Lee Y, Yoon JH, Choi JY, et al. FABP3-mediated membrane lipid saturation alters fluidity and induces ER stress in skeletal muscle with aging. Nat Commun 2020;11:5661.
PUBMED | CROSSREF

35. Pieterman CR, Conemans EB, Dreijerink KM, de Laat JM, Timmers HT, Vriens MR, et al. Thoracic and duodenopancreatic neuroendocrine tumors in multiple endocrine neoplasia type 1: natural history and function of menin in tumorigenesis. Endocr Relat Cancer 2014;21:R121-R142.
PUBMED | CROSSREF

36. Yan X, Qin C, Deng D, Yang G, Feng J, Lu R, et al. Regulation of glucose and lipid metabolism by insulin and glucagon *in vivo* and in vitro in common carp Cyprinus carpio L. Aquacult Rep 2020;18:100427.
CROSSREF

37. Patel VJ, Joharapurkar AA, Kshirsagar SG, Sutariya BK, Patel MS, Patel HM, et al. Coagonist of glucagon-like peptide-1 and glucagon receptors ameliorates kidney injury in murine models of obesity and diabetes mellitus. World J Diabetes 2018;9:80-91.
PUBMED | CROSSREF

38. Lee YH, Wang MY, Yu XX, Unger RH. Glucagon is the key factor in the development of diabetes. Diabetologia 2016;59:1372-1375.
PUBMED | CROSSREF

39. Chausmer AB. Zinc, insulin and diabetes. J Am Coll Nutr 1998;17:109-115.
PUBMED | CROSSREF

40. Panda AC, Grammatikakis I, Yoon JH, Abdelmohsen K. Posttranscriptional regulation of insulin family ligands and receptors. Int J Mol Sci 2013;14:19202-19229.
PUBMED | CROSSREF

41. Kojima S, Matsumoto K, Hirose M, Shimada M, Nagano M, Shigeyoshi Y, et al. LARK activates posttranscriptional expression of an essential mammalian clock protein, PERIOD1. Proc Natl Acad Sci U S A 2007;104:1859-1864.
PUBMED | CROSSREF

42. Burrows C, Abd Latip N, Lam SJ, Carpenter L, Sawicka K, Tzolovsky G, et al. The RNA binding protein Larp1 regulates cell division, apoptosis and cell migration. Nucleic Acids Res 2010;38:5542-5553.
PUBMED | CROSSREF

43. Stefanovic B. RNA protein interactions governing expression of the most abundant protein in human body, type I collagen. Wiley Interdiscip Rev RNA 2013;4:535-545.
PUBMED | CROSSREF

44. Gatfield D, Izaurralde E. Nonsense-mediated messenger RNA decay is initiated by endonucleolytic cleavage in Drosophila. Nature 2004;429:575-578.
PUBMED | CROSSREF

45. Kosti A, de Araujo PR, Li WQ, Guardia GD, Chiou J, Yi C, et al. The RNA-binding protein SERBP1 functions as a novel oncogenic factor in glioblastoma by bridging cancer metabolism and epigenetic regulation. Genome Biol 2020;21:195.
PUBMED | CROSSREF

46. Ahn JW, Kim S, Na W, Baek SJ, Kim JH, Min K, et al. SERBP1 affects homologous recombination-mediated DNA repair by regulation of CtIP translation during S phase. Nucleic Acids Res 2015;43:6321-6333.
PUBMED | CROSSREF

47. Batey RT, Rambo RP, Lucast L, Rha B, Doudna JA. Crystal structure of the ribonucleoprotein core of the signal recognition particle. Science 2000;287:1232-1239.
PUBMED | CROSSREF

48. Yao C, Chen Y, Wang J, Qian T, Feng W, Chen Y, et al. LncRNA BC088259 promotes Schwann cell migration through Vimentin following peripheral nerve injury. Glia 2020;68:670-679.
PUBMED | CROSSREF

49. Song KY, Choi HS, Law PY, Wei LN, Loh HH. Vimentin interacts with the 5′-untranslated region of mouse mu opioid receptor (MOR) and is required for post-transcriptional regulation. RNA Biol 2013;10:256-266.
PUBMED | CROSSREF

50. Challa AA, Stefanovic B. A novel role of vimentin filaments: binding and stabilization of collagen mRNAs. Mol Cell Biol 2011;31:3773-3789.
PUBMED | CROSSREF

51. Kourtidis A, Ngok SP, Pulimeno P, Feathers RW, Carpio LR, Baker TR, et al. Distinct E-cadherin-based complexes regulate cell behaviour through miRNA processing or Src and p120 catenin activity. Nat Cell Biol 2015;17:1145-1157.
PUBMED | CROSSREF

52. Kourtidis A, Necela B, Lin WH, Lu R, Feathers RW, Asmann YW, et al. Cadherin complexes recruit mRNAs and RISC to regulate epithelial cell signaling. J Cell Biol 2017;216:3073-3085.
PUBMED | CROSSREF

53. Hillgartner FB, Charron T, Chesnut KA. Triiodothyronine stimulates and glucagon inhibits transcription of the acetyl-CoA carboxylase gene in chick embryo hepatocytes: glucose and insulin amplify the effect of triiodothyronine. Arch Biochem Biophys 1997;337:159-168.
PUBMED | CROSSREF

54. Cozzolino C, Villani GR, Frisso G, Scolamiero E, Albano L, Gallo G, et al. Biochemical and molecular characterization of 3-Methylcrotonylglycinuria in an Italian asymptomatic girl. Genet Mol Biol 2018;41:379-385.
PUBMED | CROSSREF

55. Jitrapakdee S, Wallace JC. Structure, function and regulation of pyruvate carboxylase. Biochem J 1999;340:1-16.
PUBMED | CROSSREF

56. Agius L, Alberti KG. Regulation of flux through pyruvate dehydrogenase and pyruvate carboxylase in rat hepatocytes. Effects of fatty acids and glucagon. Eur J Biochem 1985;152:699-707.
PUBMED | CROSSREF

57. Kouchi Z. Physiological role of endocannabinoid-hydrolyzing enzymes in brain development and neurodegeneration. Biochem Physiol 2015;4:180.
CROSSREF

58. Dieckmann BW. Regulation of insulin resistance by Cyp2c44-derived lipids [master's thesis]. Nashville (TN): Vanderbilt University; 2016.

59. Hanna VS, Hafez EA. Synopsis of arachidonic acid metabolism: A review. J Adv Res 2018;11:23-32.
PUBMED | CROSSREF

60. Dyerberg J, Bang HO. Lipid metabolism, atherogenesis, and haemostasis in Eskimos: the role of the prostaglandin-3 family. Haemostasis 1979;8:227-233.
PUBMED

61. Ahmadian M, Wang Y, Sul HS. Lipolysis in adipocytes. Int J Biochem Cell Biol 2010;42:555-559.
PUBMED | CROSSREF

62. Cantini G, Trabucco M, Di Franco A, Mannucci E, Luconi M. Glucagon modulates proliferation and differentiation of human adipose precursors. J Mol Endocrinol 2019;63:249-260.
PUBMED | CROSSREF

63. Zhao L, Zhu C, Lu M, Chen C, Nie X, Abudukerimu B, et al. The key role of a glucagon-like peptide-1 receptor agonist in body fat redistribution. J Endocrinol 2019;240:271-286.
PUBMED | CROSSREF

64. Patteson AE, Vahabikashi A, Goldman RD, Janmey PA. Mechanical and non-mechanical functions of filamentous and non-filamentous vimentin. BioEssays 2020;42:e2000078.
PUBMED | CROSSREF

65. Zehmer JK, Huang Y, Peng G, Pu J, Anderson RG, Liu P. A role for lipid droplets in inter-membrane lipid traffic. Proteomics 2009;9:914-921.
PUBMED | CROSSREF

66. Aleshin AE, Yao Y, Iftikhar A, Bobkov AA, Yu J, Cadwell G, et al. Structural basis for the association of PLEKHA7 with membrane-embedded phosphatidylinositol lipids. Structure. Forthcoming 2021.
PUBMED | CROSSREF